Investigating the Gravitational Potential, the Gravity Effect and the (First and Second) Derivatives of the Gravity Effect

Fazlie Latib, *Department of Geoscience, University of Calgary*

Abstract

To understand the basic of gravity surveying, a code was developed in MATLAB to perform forward modelling for gravity anomalies in the subsurface. Two functions are built to perform the computation of U and g_z. In the first part, three sets of 5 individual masses (total mass equal to 10 million metric tonne) and their locations were generated randomly following the specified normal distribution constraints. In each set, the total gravitational potential and total gravity effect due to the contributions from each mass were computed at three different elevations of investigation point (0, 10 and 100 m). The results were plotted using three different grid spacings (5, 10 and 25 m). The results are then compared with previous investigation which uses a single mass of 1.0×10^7 kg. The results agree with each other. As the elevation of the investigation point increases, the magnitude of U and g_z decreases. Smaller grid spacing produced contour plots of U and g_z that are much more precise in terms of the resolution where it showed a better ability to resolve the mass distribution. Non-uniqueness in geophysical survey is portrayed as the mass distribution is much more difficult to resolve when the grid spacings increase. In the second part, a forward modelling is performed to generate survey results for a given anomaly data with randomly distributed density. Few density cross-sections were plotted at chosen values of x, y, and z. The total mass of the anomaly was calculated to be 4.79×10^9 kg. The gravity effect due to the density anomalies were computed at four different elevations of investigation point (0, 1, 100 and 110 m). The results at z = 0 and 100 m were plotted using three different grid spacings (5, 10 and 25 m). The first derivative of g_z, $\partial g/\partial z$ at z = 0 and 100 m were estimated using the gravity effect computed earlier and were plotted using three different grid spacings (5, 10 and 25 m). The resolution of $\partial g/\partial z$ contour plots is much better with a small grid spacings and a lower survey elevation. The second derivative of g_z, $\partial^2 g/\partial z^2$ at z = 0 and 100 m is estimated using the gravity effect at z = 0 and 100 m. Three different grid spacings (5, 10 and 25 m) were used to plot $\partial^2 g/\partial z^2$ at z = 0 and 100 m. Once again, the resolution also decreases here as the spacings increases.

Background / Theory

Gravity method is a versatile geophysical technique used to detect and identify subsurface bodies and anomalies within the Earth. This method has been used extensively in the hydrocarbon and mineral exploration over the years. Gravity surveys exploit the very small changes in gravity from place to place that are caused by changes in subsurface rock density (Telford et al., 1990). Higher gravity values are found over rocks that are denser, and lower gravity values are found over rocks that are less dense. A buried body represents a subsurface zone of anomalous mass and causes a localized perturbation in the gravitational field known as a gravity anomaly. The basis of the gravity method is Newton's Law of Gravitation, which states that the force of attraction, F, between two masses (m_1 and m_2) is directly proportional to the product of the two masses and inversely proportional to the square of the distance between their centres of mass. The greater the distance separating the centres of mass, the smaller is the force of attraction between them.

The gravitational potential, U, due to a concentrated point mass, m, is given by Equation 1 where $G \approx 6.674 \times 10^{-11}$ N m^2 kg^{-2} is the universal constant of gravitation, and r is the distance from the mass. To calculate U at a point, $\mathrm{x} = x\hat{\mathbf{i}} + y\hat{\mathbf{j}} + z\hat{\mathbf{k}}$ due to a mass at $\mathrm{x_m} = x_m\hat{\mathbf{i}} + y_m\hat{\mathbf{j}} + z_m\hat{\mathbf{k}}$, the distance between them first needs to be computed using Equation 2 where $\hat{\mathbf{i}}$, $\hat{\mathbf{j}}$, and $\hat{\mathbf{k}}$ are the standard unit vectors in the direction of the x, y, and z axes. Generally, U represents the gravitational potential at a distance r from mass m.

$$U = \frac{Gm}{r} \tag{1}$$

$$r = \|\mathrm{x} - \mathrm{x_m}\| = \sqrt{(x - x_m)^2 + (y - y_m)^2 + (z - z_m)^2} \tag{2}$$

The principal component of gravity measured by gravimeters and used in most gravity analyses is in the vertical direction, hence, the gravity effect, g_z, can be derived from Equation 1 by finding the first derivative of U with respect to z. The first step in finding the equation for g_z is by using a chain rule (Equation 3). By solving the chain rule, g_z is finally given by Equation 4. Equation 4 calculates the gravity effect where the mass anomaly is treated as a point source or mass. However, the physical subsurface of the Earth is much more dimensional than that. Rather, the anomalies will tend to have varying body dimensions (irregular shape) with non-uniform densities. To account for that, the gravity effect due to an arbitrary mass of known density, ρ, in the subsurface can be calculated if the differential mass, dm, contained in a differential volume, dV, is estimated using Equation 5.

$$g_z = -\frac{\partial U}{\partial z} = -\frac{\partial U}{\partial r} \cdot \frac{\partial r}{\partial z} \tag{3}$$

$$g_z = -\left(-\frac{Gm}{r^2}\right)\left(\frac{1}{2}(r^{-0.5})\big(2(z - z_m)\big)\right) = \left(\frac{Gm}{r^2}\right)\left(\frac{z - z_m}{r}\right) = Gm\frac{z - z_m}{r^3} \tag{4}$$

$$dm = \rho\, dV \tag{5}$$

The first derivatives of g_z, $\partial g/\partial z$ is the difference in the gravity effect divided by the different in depths between two points and can be calculated using Equation 6. This information is used to observe anomalies by comparing measured values of $\partial g/\partial z$ with a reference model of the Earth's gravity at a particular location. It is possible to measure $\partial g/\partial z$ by taking measurements over the same region at different altitudes. However, duplicating a survey over the same region at different altitudes may be technically challenging even for airborne or satellite surveys, so measurements of $\partial g/\partial z$ in practice are uncommon.

$$\frac{\partial g}{\partial z} = \frac{\Delta g}{\Delta z} = \frac{g_1 - g_0}{z_1 - z_0} \tag{6}$$

Differentiating again with respect to z gives the second vertical derivative of g_z, $\partial^2 g/\partial z^2$. Unlike $\partial g/\partial z$, $\partial^2 g/\partial z^2$ can be obtained from a single survey since g_z satisfies the Laplace equation (Equation 7). Rearranging Equation 7 into Equation 8, $\partial^2 g/\partial z^2$ can be estimated by computing the derivatives of g in the lateral directions (x and y directions). The first derivatives in the x and y directions using a central difference are shown in Equation 9 and 10 respectively where it measures the first derivative estimates at the midpoints between the grid points with measured values of g. Applying again the central difference to the first derivative (Equation 9 and 10), the second derivatives in the x and y directions can be calculated using Equation 11 and 12. Vertical derivatives tend to magnify values at small z (shallow depth) at the expense of values at large z. Hence, calculating $\partial^2 g/\partial z^2$ is useful for isolating near surface anomalies.

$$\nabla^2 g = \frac{\partial^2 g}{\partial x^2} + \frac{\partial^2 g}{\partial y^2} + \frac{\partial^2 g}{\partial z^2} = 0 \tag{7}$$

$$\frac{\partial^2 g}{\partial z^2} = -\left(\frac{\partial^2 g}{\partial x^2} + \frac{\partial^2 g}{\partial y^2}\right) \tag{8}$$

$$\left(\frac{\partial g}{\partial x}\right)_{i,j-\frac{1}{2}} = \frac{g_{i,j} - g_{i,j-1}}{\Delta x} \tag{9}$$

$$\left(\frac{\partial g}{\partial y}\right)_{i-\frac{1}{2},j} = \frac{g_{i,j} - g_{i-1,j}}{\Delta y} \tag{10}$$

$$\left(\frac{\partial^2 g}{\partial x^2}\right)_{i,j} = \frac{\left(\frac{\partial g}{\partial x}\right)_{i,j+\frac{1}{2}} - \left(\frac{\partial g}{\partial x}\right)_{i,j-\frac{1}{2}}}{\Delta x} = \frac{\left(\frac{g_{i,j+1} - g_{i,j}}{\Delta x}\right) - \left(\frac{g_{i,j} - g_{i,j-1}}{\Delta x}\right)}{\Delta x}$$
$$= \frac{g_{i,j+1} - 2g_{i,j} + g_{i,j-1}}{\Delta x^2} \tag{11}$$

$$\left(\frac{\partial^2 g}{\partial y^2}\right)_{i,j} = \frac{g_{i+1,j} - 2g_{i,j} + g_{i-1,j}}{\Delta y^2} \tag{12}$$

Methods / Algorithm

The algorithm comprises of two main functions. The first function, **grav_pot_point()**, computes the gravitational potential due to a mass anomaly using Equation 1 while the second function, **grav_eff_point()**, computes the gravity effect of the mass anomaly using Equation 4. Both the functions take as inputs a vector containing the coordinates at which U and g_z is to be computed, a vector containing the coordinates of the location of the point mass, x, the mass of the anomaly, m, and the universal constant of gravitation, G. The functions gave outputs as U and g_z values respectively.

Part 1

Three different sets of 5 masses at different locations were generated with the total mass of each set is equal to 10 million metric tonne ($m = \sum_{i=1}^{5} m_i = 1.0 \times 10^7$ kg) and the location of their centre of mass is located at x = $0\hat{\mathbf{i}}$ + $0\hat{\mathbf{j}}$ - $10\hat{\mathbf{k}}$. The first four masses and their locations are generated randomly using MATLAB function **randn()** from a normal distribution where $\mu_m = m/5$, $\sigma_m = m/100$, $\mu_x = \mu_y = 0$ m, $\mu_z = -10$ m, $\sigma_x = \sigma_y = 20$ m and $\sigma_z = 2$ m (μ_i and σ_i are the mean and standard deviation of the distribution of i). The fifth mass is found using Equation 13 while its location is then computed using the first four masses' locations and all five masses so that it satisfies the constraints in Equation 14 (the location is found by rearranging Equation 14 into Equation 15).

$$m_5 = m - (m_1 + m_2 + m_3 + m_4) \tag{13}$$

$$\begin{Bmatrix} \bar{x} \\ \bar{y} \\ \bar{z} \end{Bmatrix} = \frac{1}{m} \begin{Bmatrix} \sum_{i=1}^{5} m_i x_i \\ \sum_{i=1}^{5} m_i y_i \\ \sum_{i=1}^{5} m_i z_i \end{Bmatrix} = \begin{Bmatrix} 0 \\ 0 \\ -10 \end{Bmatrix} \text{m} \tag{14}$$

$$\begin{Bmatrix} x_5 \\ y_5 \\ z_5 \end{Bmatrix} = \begin{Bmatrix} -\dfrac{m_1 x_1 + m_2 x_2 + m_3 x_3 + m_4 x_4}{m_5} \\ -\dfrac{m_1 y_1 + m_2 y_2 + m_3 y_3 + m_4 y_4}{m_5} \\ \dfrac{-10m - (m_1 x_1 + m_2 x_2 + m_3 x_3 + m_4 x_4)}{m_5} \end{Bmatrix} \text{m} \tag{15}$$

MATLAB function **meshgrid()** is used to build a grid with regular spacings (grid spacings of 5, 10 and 25 m is used) that runs from $x_{min} = y_{min} = -100$ m to $x_{max} = y_{max} = +100$ m. Nested for loop is then utilized to calculate the total potential, U, and the total gravity effect, g_z, for each mass set at each point in the grid by summing the contributions of U and g_z from each individual mass in the set where the contributions are calculated using **grav_pot_point()** and **grav_eff_point()** functions respectively. The U and g_z at three different elevations (z = 0, 10 and 100 m) were calculated and contour plots of U and g_z are built using MATLAB function **contourf()**. MATLAB function **subplot()** is used to show the plots on a subplot grid with 2 columns (one for U and one for g_z) and 3 rows (one for each z value).

Part 2

An anomaly file provided, **'anomaly_data.mat'**, contains four arrays (**x**, **y**, **z** and **rho**). The details of the geometry and density distribution of an anomaly is provided by the data file. For some set of indices **{i,j,k}**, the vector **[x(i,j,k), y(i,j,k), z(i,j,k)]** gives the coordinates of a point in the subsurface and **rho(i,j,k)** gives the density of the material near that point. The grid spacing is 2 m, so each point is at the centre of a small cube with volume of 2 m × 2 m × 2 m = 8 m^3.

To visualize the distribution of the density of the anomaly, multiple cross-sections were produced. The density cross-sections of the anomaly at z = {-8, -10, -12}m, y = {-8, 0, 8}m and x = {-16, 0, 16}m were generated using **contourf()**. **subplot()** is used to show the plots on a subplot grid with 3 columns (one for each x, y and z) and 3 rows (each value in x, y and z). For values of x, y, and z, the location of **i**, **j**, and **k [x(i,j,k), y(i,j,k), z(i,j,k)]** is searched respectively from the anomaly data. For example, to build a cross-section at z = -8 m, the location of **k** in **[x(i,j,k), y(i,j,k), z(i,j,k)]** where k = -8 is searched using MATLAB function **find()**. After the location of **k** is found, the density cross section can be plotted.

meshgrid() is used to build a grid with regular spacings (grid spacings of 5, 10 and 25 m is used) that runs from $x_{min} = y_{min}$ = -100 m to $x_{max} = y_{max}$ = +100 m. To forward model what a ground-based survey and an airborne survey would look like for this anomaly, nested for loop is utilized to calculate the total gravity effect, g_z, due to the density anomaly at each point in the grid by summing the contributions of g_z from the irregular anomaly where the contributions of the non-zero density are calculated using **grav_eff_point()** function. The mass used in the function is calculated using Equation 5. The g_z at two different elevations, z = 0 (ground-based survey) and z = 100 m (airborne survey) were calculated and contour plots of g_z are built using **contourf()**. **subplot()** is used to show the plots on a subplot grid with 3 columns (one for each grid spacings) and 2 rows (one for each z value). Using the same nested loop, the total mass of the density anomalies are computed.

To approximate $\partial g/\partial z$ at z = 0 m and z = 100 m, another set of survey results for g_z at z = 1 m and z = 110 m were obtained following the same steps above. Using Equation 6 and g_z values (at z = 0, 1, 100 and 110 m), $\partial g/\partial z$ at z = 0 m and z = 100 m are calculated where the first point is at z = 1 m and z = 110 m respectively and the second point is at z = 0 m and z = 100 m respectively. The contour plots of $\partial g/\partial z$ at z = 0 m and z = 100 m are built using **contourf()**. **subplot()** is used to show the plots on a subplot grid with 3 columns (one for each grid spacings) and 2 rows (one for each z value).

Using Equation 11 and 12 with the g_z values at z = 0 m and z = 100 m in a nested while loop, $\partial^2 g/\partial x^2$ and $\partial^2 g/\partial y^2$ at z = 0 m and z = 100 m were calculated. Then, $\partial^2 g/\partial z^2$ at z = 0 m and z = 100 m can be calculated using Equation 8. The contour plots of $\partial^2 g/\partial z^2$ at z = 0 m and z = 100 m are built using **contourf()**. **subplot()** is used to show the plots on a subplot grid with 3 columns (one for each grid spacings) and 2 rows (one for each z value).

Results and Discussion

Part 1

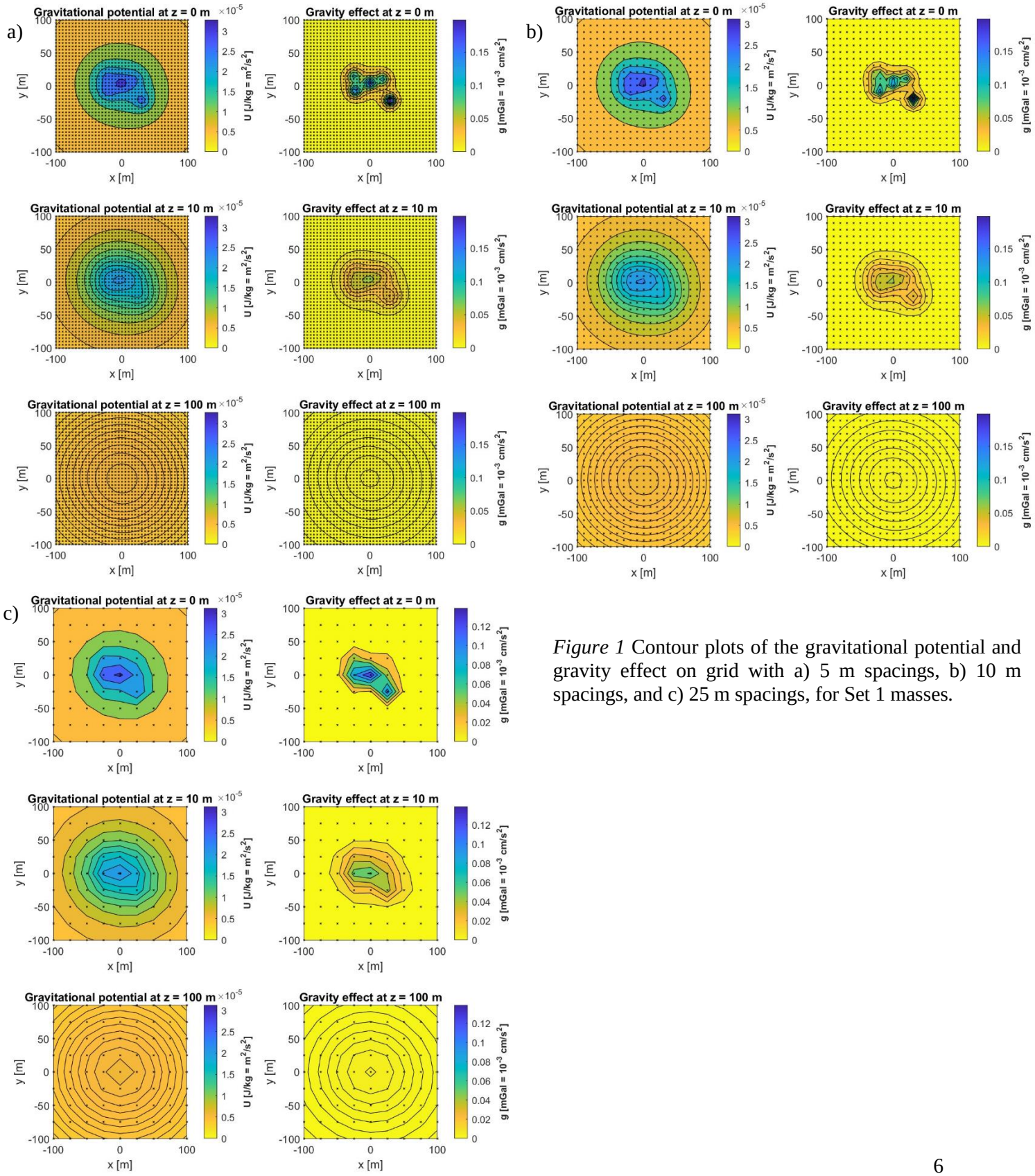

Figure 1 Contour plots of the gravitational potential and gravity effect on grid with a) 5 m spacings, b) 10 m spacings, and c) 25 m spacings, for Set 1 masses.

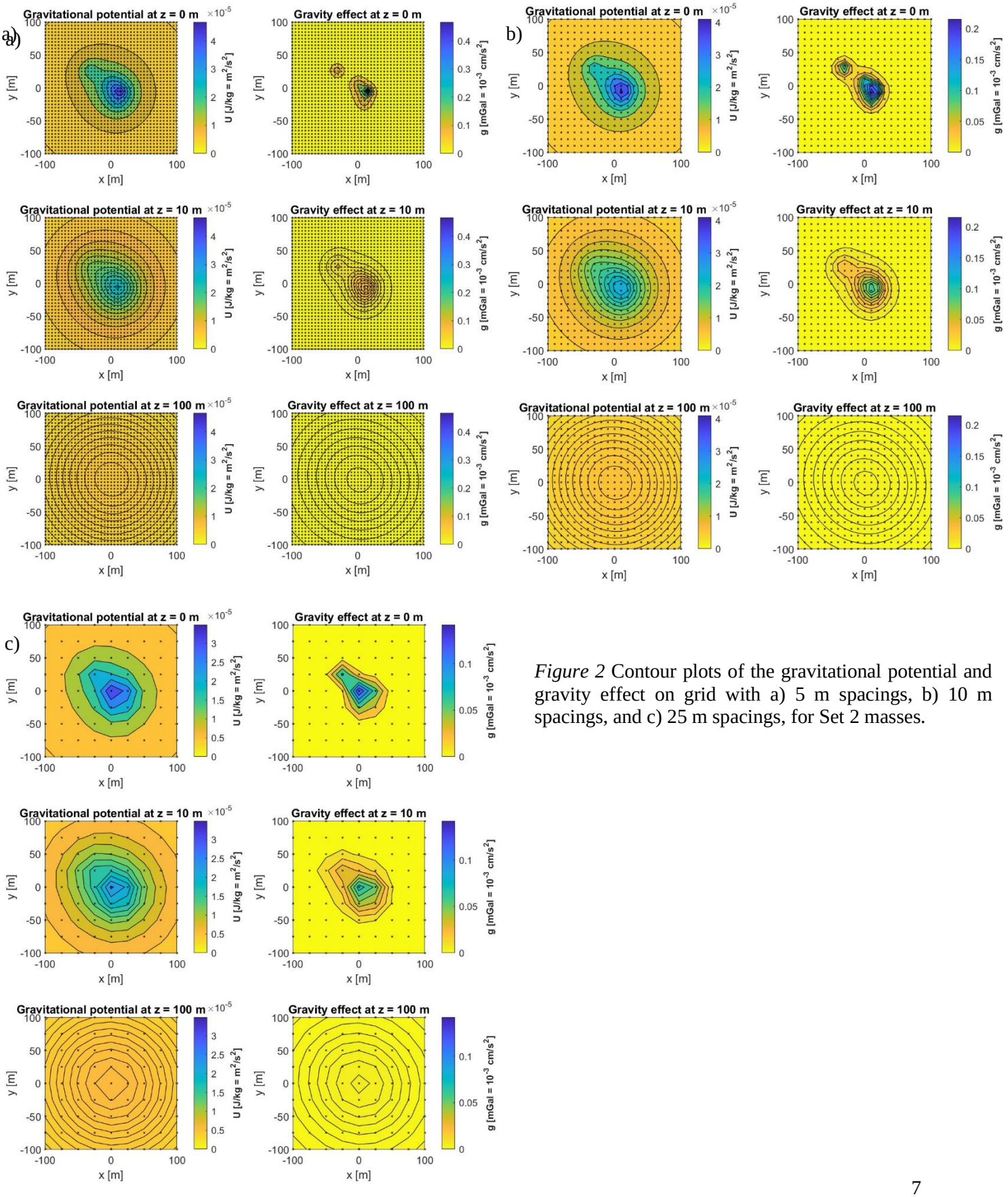

Figure 2 Contour plots of the gravitational potential and gravity effect on grid with a) 5 m spacings, b) 10 m spacings, and c) 25 m spacings, for Set 2 masses.

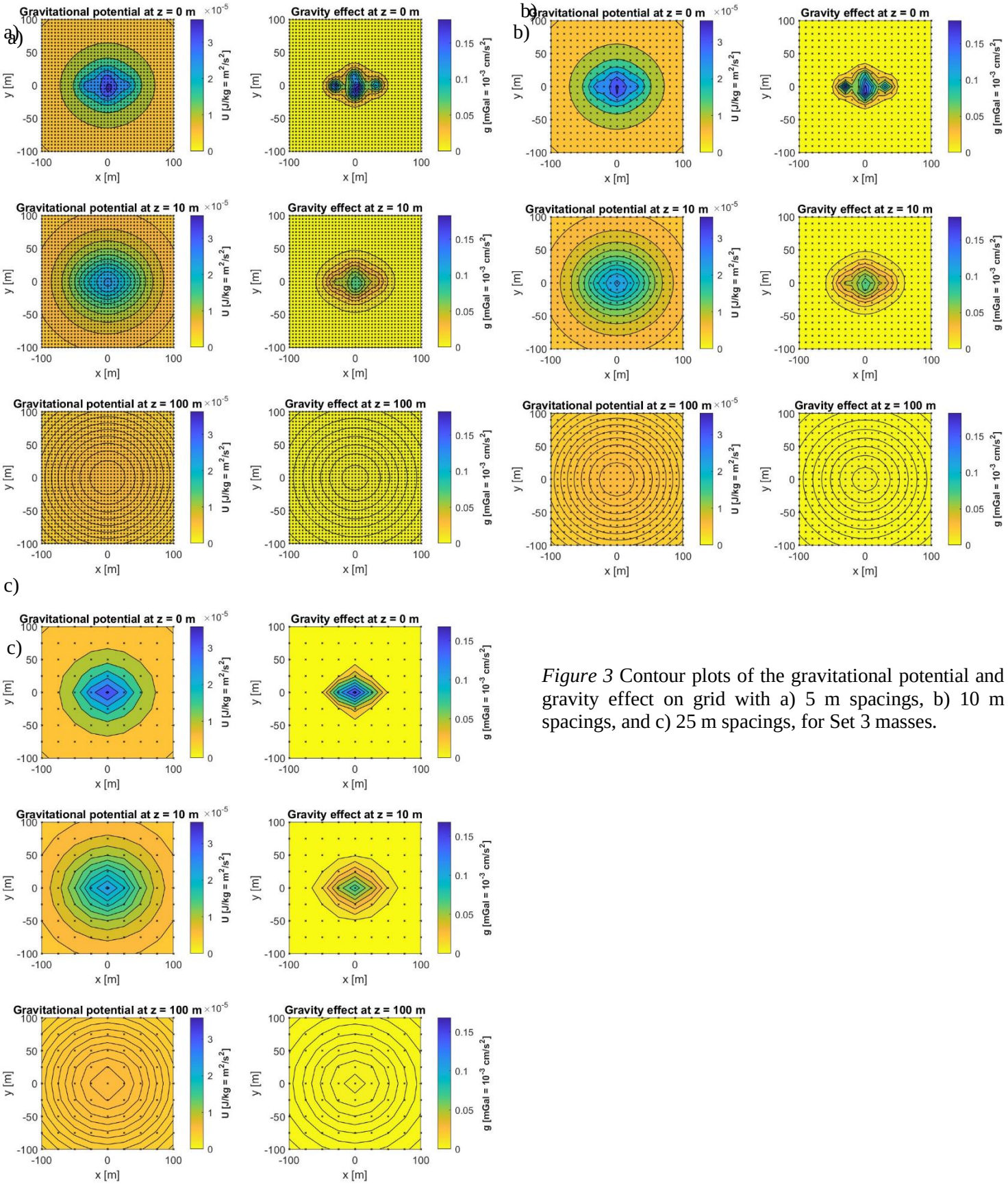

Figure 3 Contour plots of the gravitational potential and gravity effect on grid with a) 5 m spacings, b) 10 m spacings, and c) 25 m spacings, for Set 3 masses.

From Figure 1, the maximum total gravitational potential and gravity effect from Set 1 masses (represented by dark blue area in the contour plots) can be found when z = 0 m where the values are around 3.3×10^{-5} m^2 $/s^2$ and 0.2 mGal respectively. As the elevation of investigation is increased to 10 m, the total maximum gravitational potential and gravity effect decreased to around 2.0×10^{-5} m^2 $/s^2$ and 0.075 mGal respectively. As we increased the elevation again, this time to a 100 m, both the gravitational potential and gravity effect decreased much more where the values are around 0.5×10^{-5} m^2 $/s^2$ and 0-0.01 mGal respectively. The same pattern can be seen when masses of Set 2 and 3 were used as shown in Figure 2 and 3. Hence, U and g_z decrease as z increases. Analogously, if only a ground-based gravity survey ($z = 0$ m) is done for the same mass anomaly but at a much deeper depth, the gravitational potential and gravity effect would decrease. These results agreed with the results obtained from previous investigation using a single mass of $m = 1 \times 10^7$ kg.

The difference between the randomly distributed mass and the single mass is that the values of U and g_z are no longer decreasing from one single point but instead there were few points from where the contour plots started decreasing. This is because the different masses in each set would contribute to U and g_z differently across the grid. However, this can only be observed at $z = 0$ m with the smallest spacings which is 5 m. As the spacings were increased, the resolution of the contour plots became less precise where the gradual changes across the contour plot becomes less smooth making the ability to resolve the mass distribution decreased. Hence, smaller grid spacings help resolve the anomalies better. This is very evident as we observed the changes of the contour plot of U and g_z at $z = 0$ m in Figure 3 (Set 3) as the grid spacings increased from 5 m to 10 m to 25 m where the distribution of mass in Set 3 becomes much harder to resolve. This difficulty in resolving masses is an example of non-uniqueness in geophysical surveying. The effect of grid spacings is the same with the single mass results. In other words, as the grid spacings increase, the quality of the contour plot output decreases.

Part 2

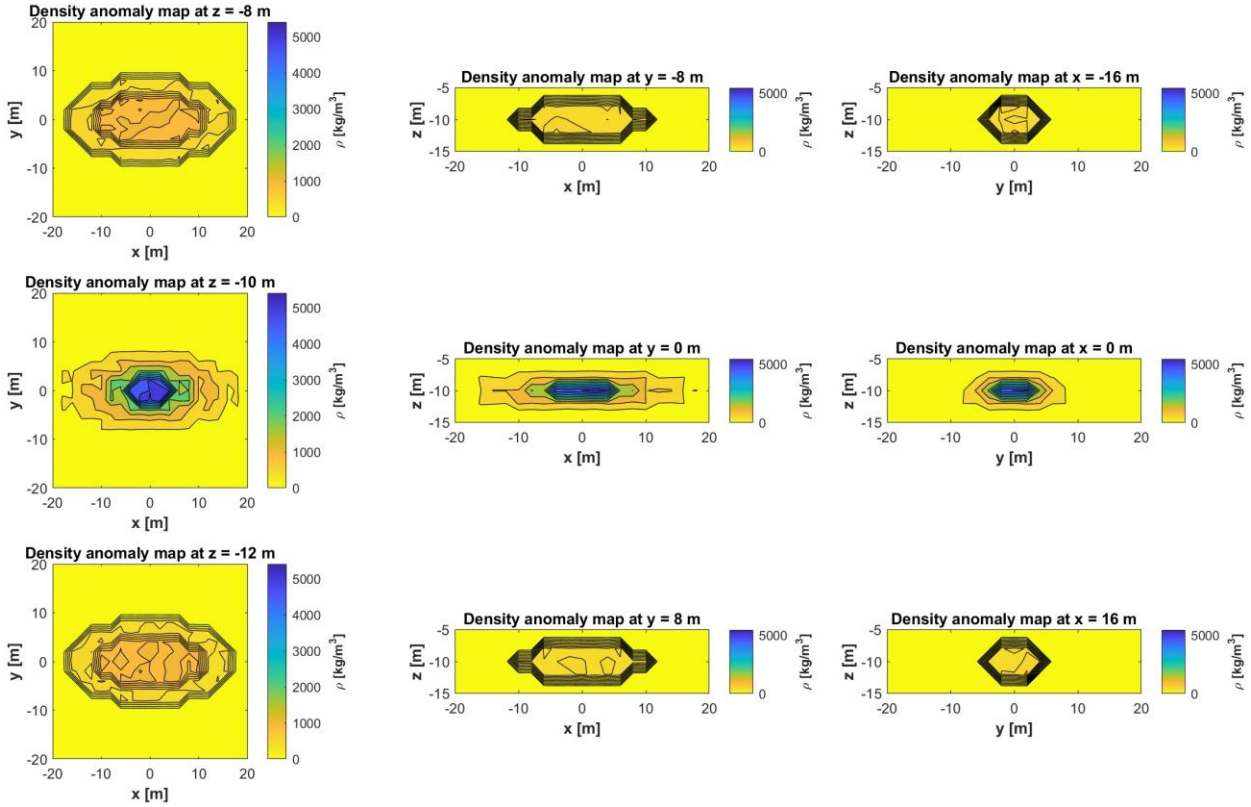

Figure 4 Contour plots of the density cross-sections at selected values of *z*, *y* and *x*.

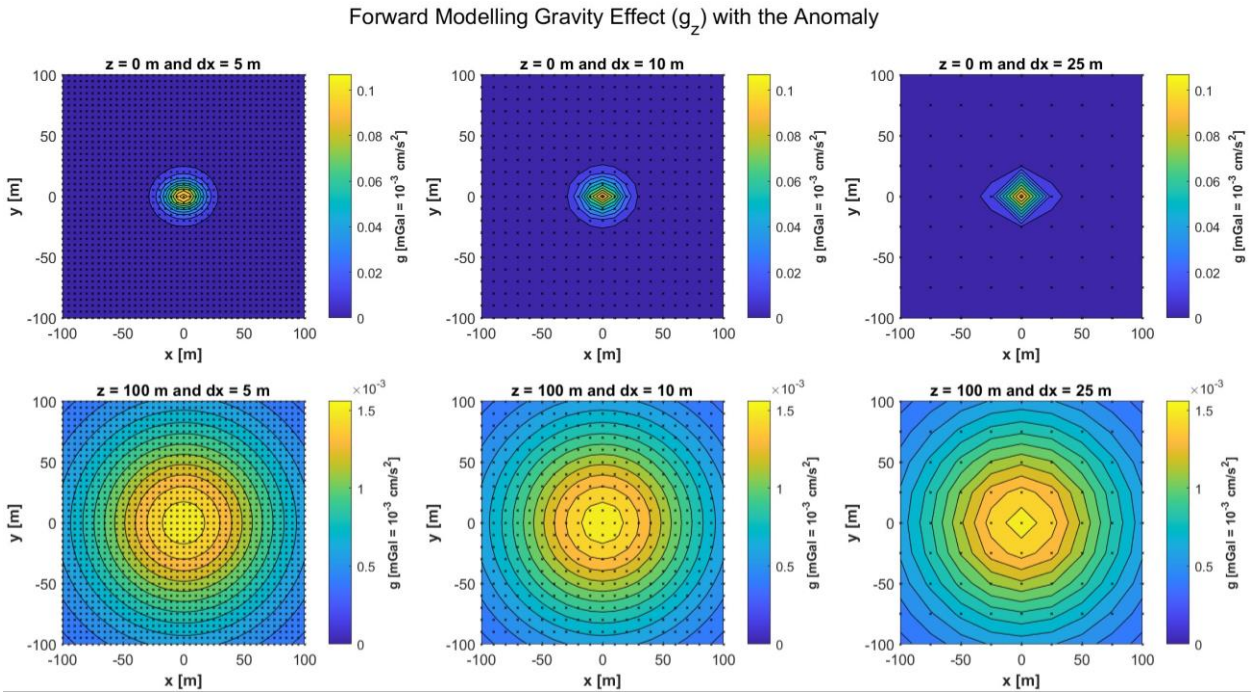

Figure 5 Contour plots of the forward model of gravity effect for the anomaly at *z* = 0 and 100 m at three different spacings.

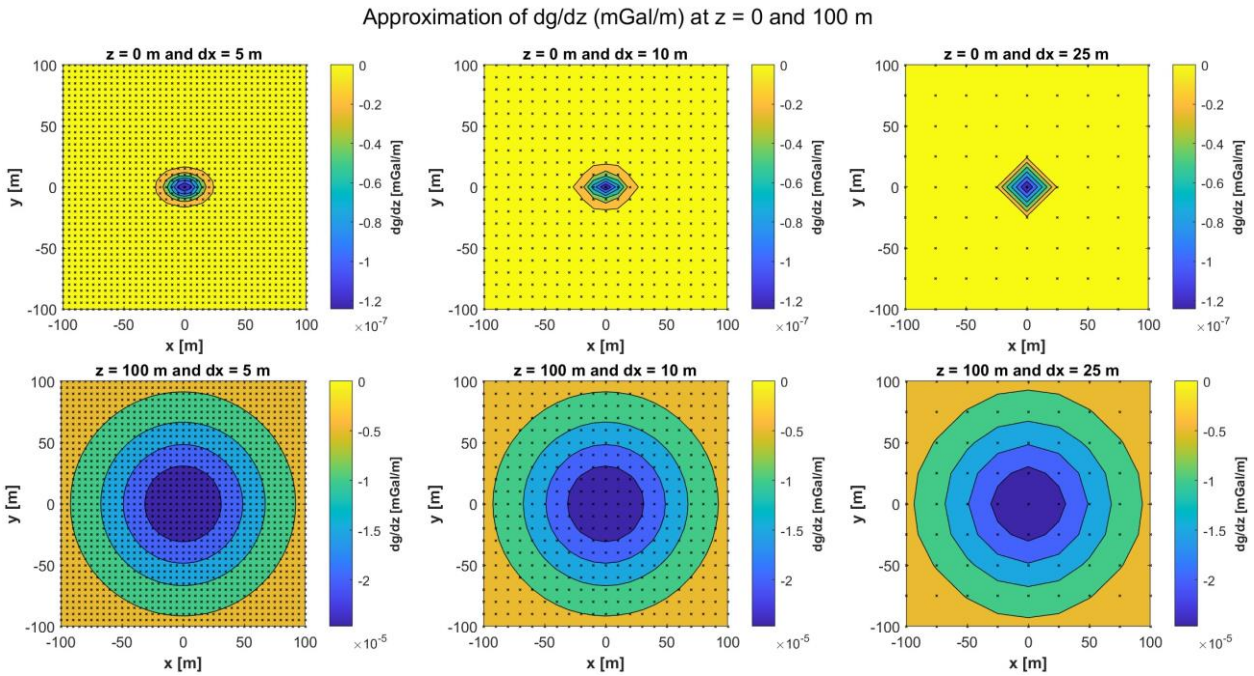

Figure 6 Contour plots of approximation of $\partial g/\partial z$ for the anomaly at z = 0 and 100 m at three different spacings.

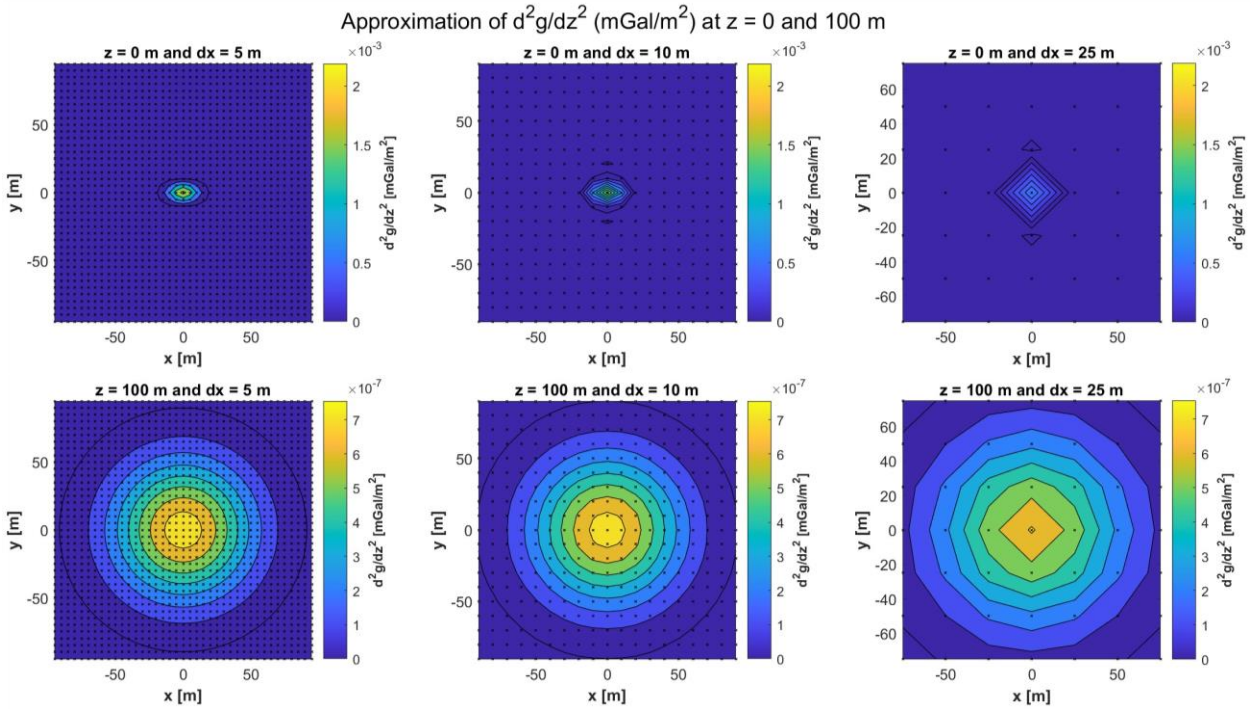

Figure 7 Contour plots of approximation of $\partial^2 g/\partial z^2$ for the anomaly at z = 0 and 100 m at three different spacings.

In Figure 4, the density cross-sections of a given anomaly data with randomly distributed densities were plotted at chosen values of x, y and z. These cross-sections correlate better to a real-world example of the subsurface. The maximum density (represented by dark blue area in the contour plots) can be found on density cross-sections at x = 0 m, y = 0 m, and z = -10 m where the value is around 5000 kg/m^3. The total mass of the anomaly was calculated to be 4.79×10^9 kg.

In Figure 5, the forward model of a ground-based survey (z = 0 m) and an airborne survey (z = 100 m) for the anomaly is shown. The maximum gravity effect for the ground-based survey is around 0.1 mGal which is much higher than maximum gravity effect for the airborne survey which is around 1.6×10^{-3} mGal. As in the figures in Part 1, the resolution in Figure 5 decreases as the grid spacings widened.

The first derivative of g_z, $\partial g/\partial z$ at z = 0 m and z = 100 m is plotted in Figure 6. The magnitude of $\partial g/\partial z$ at z = 0 m is smaller than $\partial g/\partial z$ at z = 100 m by a 10^2 magnitude. The resolution decreases as the spacings increases especially for $\partial g/\partial z$ at z = 0 m where at 5 m spacings, $\partial g/\partial z$ with high magnitude is well defined by an oval (no-edge) area but at higher spacings (25 m), the area of high magnitude becomes more edgy (square shape). For $\partial g/\partial z$ at z = 100 m, the resolution is not much affected by the increase in grid spacings but the sensitivity in estimating $\partial g/\partial z$ decreases as the values of $\partial g/\partial z$ is much bigger than at z = 0 m.

The second derivative of g_z, $\partial^2 g/\partial z^2$ at z = 0 m and z = 100 m is plotted in Figure 7. The magnitude of $\partial^2 g/\partial z^2$ at z = 0 m is larger than $\partial^2 g/\partial z^2$ at z = 100 m by a 10^4 magnitude. The resolution decreases as the spacings increases especially for $\partial^2 g/\partial z^2$ at z = 0 m where at 5 m spacings, the maximum value of $\partial^2 g/\partial z^2$ is around 1.5×10^{-3} mGal/m^2 but at higher spacings (25 m), the maximum is reduced to around 1×10^{-3} mGal/m^2. So, the resolution decreases as the spacings increases.

Conclusion

The gravitational potential and gravity effect due to a mass anomaly changes as we change the elevation of the investigation point. The higher the elevation point, the more the gravitational potential and gravity effect decreases. In all the contour plot showing gravitational potential, gravity effect, first and second derivatives of gravity effect, the resolution or quality of the plot decreases as the grid spacings increases.

References

Telford, W.M., Geldart, L.P., Sheriff, R.E. and Keys, D.A. (1990) Applied Geophysics (2nd edn), Cambridge